Four-Port Microwave Networks With Intrinsic Broad-Band Suppression of Common-Mode Signals

Wael M. Fathelbab, *Member, IEEE,* and Michael B. Steer, *Fellow, IEEE*

Abstract—Two classes of four-port microwave networks are defined with discriminative even- and odd-mode transmission characteristics. Design of the networks is based on filter prototypes with predefined sets of transmission zeros and, consequently, a desired response can be synthesized. A configuration consisting of a pseudodifferential active circuit in cascade with either class results in a sub-system with high common-mode rejection ratio over a broad frequency range. A pseudodifferential circuit implementation demonstrated low common-mode gain over a 3 : 1 operating bandwidth ranging from 250 to 750 MHz.

Index Terms—Common-mode signals, four-port networks, matching/filtering, pseudodifferential circuits, transmission zeros.

I. INTRODUCTION

DIFFERENTIAL circuit design leads to stable, noise-tolerant monolithically integrated analog circuits and is compatible with current-mode biasing. Symmetrical differential circuits are generally less sensitive to component variations and when appropriately designed can reject common-mode signals, particularly coupled noise. However pseudodifferential circuits, as shown, for example, in the dotted box in Fig. 1(a), typically have a unit common-mode rejection ratio (CMRR) when biased by a pair of inductors, but will have dynamic range larger than that of fully differential circuits as the constant current source is mostly eliminated. A new coupled-line based biasing scheme for pseudodifferential RF circuits leading to enhanced CMRR was recently proposed [1]. A central attribute of coupled lines is the ability to discriminate between odd and even modes and, in terms of the subject of this paper, between common- and differential-mode signals. This paper extends the biasing scheme to one based on filter prototypes and circuit synthesis procedures. In particular, two classes of four-port networks are introduced that are suited to biasing differential circuits and obtaining broad-band common-mode signal suppression.

A sub-system schematic of a pseudodifferential circuit in cascade with a four-port network connected to single-ended loads R_L is illustrated in Fig. 1. The four-port network ideally presents distinct common- and differential-mode impedances to the active devices and has the following properties:

- inherent broad-band isolation or attenuation of common-mode signals, as well as broad-band matching of differential-mode signals;
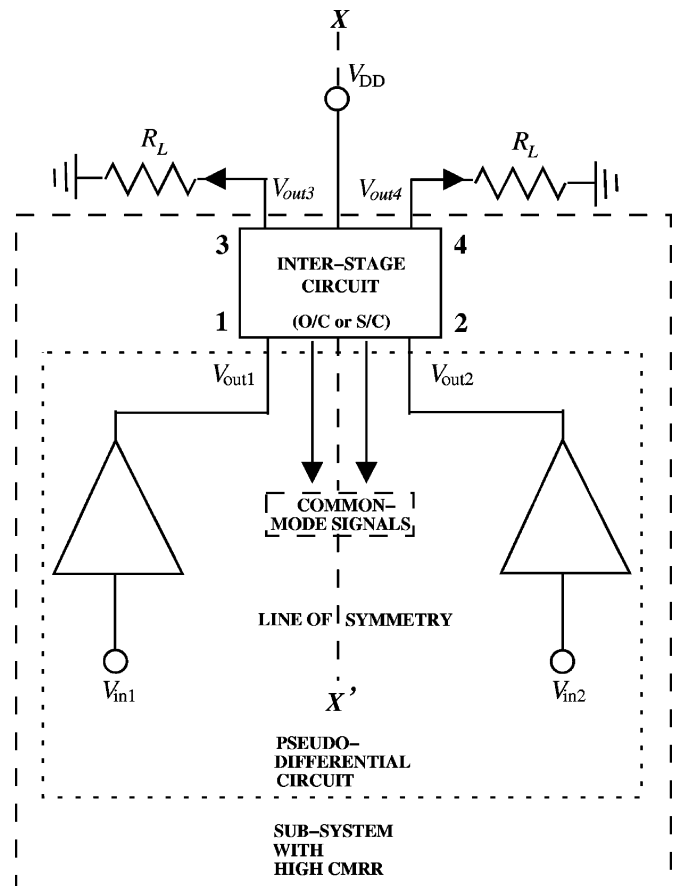
Fig. 1. Pseudodifferential circuit connected to a pair of single-ended loads R_L separated by a four-port inter-stage network. Drain voltage V_{DD} is applied at relevant points within the inter-stage network to bias the active devices.

- provides external dc biasing to the active devices.

From a circuit synthesis perspective, the first requirement necessitates that the network possesses significantly different even- and odd-mode transmission characteristics. This is essentially the rationale behind the solutions introduced in this paper. The second requirement is satisfied by appropriate selection of the set of transmission zeros of the odd-mode sub-network of the four-port inter-stage circuit.

In Section II, two classes of microwave networks with the aforementioned characteristics are presented, while in Section III, each network class is, in turn, implemented and cascaded with a pseudodifferential amplifier. Broad-band suppression of common-mode signals is demonstrated.

II. FOUR-PORT INTER-STAGE NETWORKS

Presentation of the new network classes will now commence.
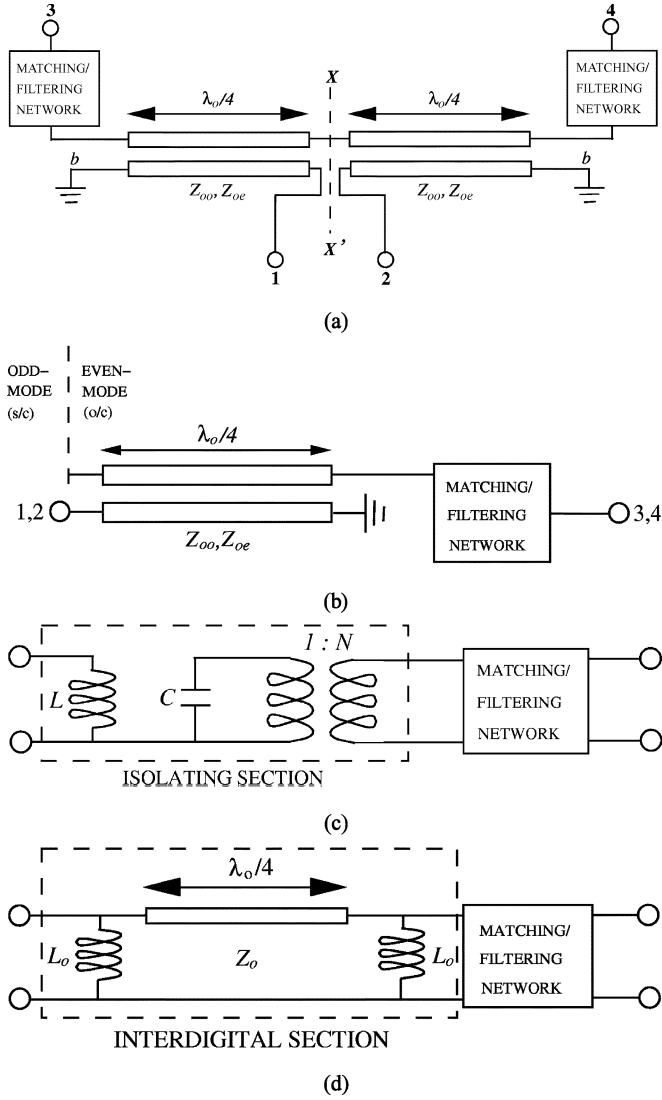
Fig. 2. Generalized topology of Class-A inter-stage network made of two pairs of coupled lines and matching/filtering networks. (a) Physical topology. (b) Even- and odd-mode sub-networks. (c) Even-mode prototype. (d) Odd-mode prototype with at least one zero at dc, and a single UE.

A. Class-A Network

The first class, denoted Class A, is shown in Fig. 2(a) and here comprises a pair of coupled-line sections connected to a pair of matching or filtering networks. The topology of the matching/filtering network is arbitrary and may consist of coupled-line sections, transmission lines, and lumped components dependent on the choice of transmission zeros required to satisfy a particular electrical specification. Application of the modal analysis to this structure results in the sub-networks of Fig. 2(b) with equivalent even- and odd-mode prototypes, as shown in Fig. 2(c) and (d), respectively. These equivalent prototypes result because the plane of symmetry $X - X'$ transforms to either an open or short circuit for common- or differential-mode signal excitations, respectively, at Ports 1 and 2. In the odd-mode effective network, differential-mode signals are passed to single-ended loads R_L, whereas in the even-mode equivalent circuit, it is seen that common-mode signals do not pass through the network by virtue of the effective series open

circuit present in the circuit. Thus, the operation of Class-A inter-stage networks in suppressing common-mode signals relies on the isolating property of the microwave section shown in the dashed box in Fig. 2(c) [6], [7]. Class-A networks also possess short-circuited points marked $\boldsymbol{b}$ in Fig. 2(a) where dc bias of the active devices can be applied with the use of decoupling capacitors.

The square of the modulus of the transmission transfer function of the reciprocal odd-mode network of Fig. 2(d) may now be defined in terms of its characteristic polynomial $K(S)$ as

$$|S_T(S)|^2_{\text{ODD}} = \frac{1}{1 + |K^2(S)|} \tag{1}$$

where $|S_T(S)|^2_{\text{ODD}}$ replaces $|S_{31}(S)|^2_{\text{ODD}}$ or $|S_{42}(S)|^2_{\text{ODD}}$. With the even-mode network, ideally there is no transmission through the network and, thus, the design objective is

$$|S_T(S)|^2_{\text{EVEN}} = 0 \tag{2}$$

where $|S_T(S)|^2_{\text{EVEN}}$ replaces $|S_{31}(S)|^2_{\text{EVEN}}$ or $|S_{42}(S)|^2_{\text{EVEN}}$. In (1) and (2), S is the Richards variable [5] defined as $j \tan((\pi/2)(f/f_r))$, where f is the real frequency variable, and f_r is the resonant frequency of the transmission-line resonators. Now the square of the modulus of the CMRR of the four-port inter-stage network may be defined as

$$|\text{CMRR}(S)|^2 = \frac{|S_T(S)|^2_{\text{ODD}}}{|S_T(S)|^2_{\text{EVEN}}} \tag{3}$$

and, consequently, the resulting CMRR of the sub-system configuration consisting of the pseudodifferential circuit in cascade with the four-port inter-stage network [the dashed box in Fig. 1(a)] is

$$\text{CMRR}(S) = \frac{\big(A_d(S)\big) \cdot \big(|S_T(S)|_{\text{ODD}}\big)}{\big(A_c(S)\big) \cdot \big(|S_T(S)|_{\text{EVEN}}\big)} \tag{4}$$

where $A_c(S)$ and $A_d(S)$ are the single-ended common- and differential-mode gains, respectively, of the pseudodifferential circuit. For a pseudodifferential circuit, $A_c(S)$ and $A_d(S)$ are identical [1] and, thus, the sub-system CMRR is dominated by the performance of the inter-stage network.

An example of a Class-A inter-stage network is illustrated in Fig. 3. It consists of a $2n$th-order network where n is the number of resonators in either the even- or odd-mode sub-networks. It is seen that the nth resonators of the even-mode prototype [see Fig. 3(b)] are completely decoupled from each other, thus offering optimum isolation of common-mode signals. On the other hand the odd-mode prototype, shown in Fig. 3(c), consists of cascades of short-circuited interdigital coupled-line sections [2]–[5], [7] loaded by open-circuited stubs. The odd-mode network [4] will possess a zero at dc, n zeros at infinity, and $(n - 1)$ zeros at $S = 1$ leading to the existence of $(n - 1)$ quarter-wave-long transmission lines (also known as unit elements (UEs) [5]).

The general design procedure of an inter-stage network starts with the synthesis of an nth-order S-plane odd-mode prototype corresponding to an f-plane response with a specific passband centered at f_o with lower and upper band-edge frequencies f_1,

(a)

(b)

(c)
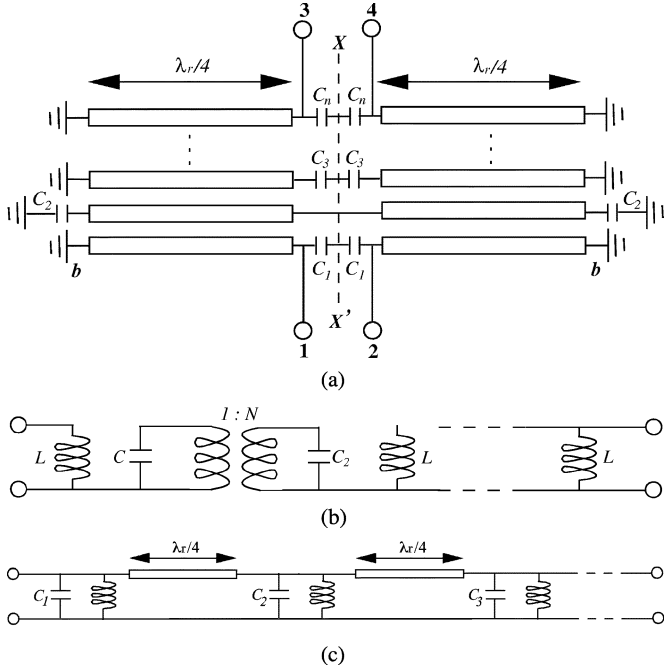
Fig. 3. Example of Class-A inter-stage network made of a pair of appropriately connected bandpass interdigital filters. (a) Physical topology. (b) Even- and (c) odd-mode prototypes.

Fig. 4. Quadrature hybrid coupler. (a) Physical topology. (b) Even- and (c) odd-mode prototypes.

and f_2, respectively, and a commensurate frequency f_r. A set of transmission zeros selected to suit a particular electrical specification with a minimum of one zero at dc and a UE may be chosen to generate the appropriate characteristic polynomial [4], [10], [11] after which the square of modulus of the reflection coefficient of the odd-mode prototype is constructed. Based on the assumption of a lossless system, the square of modulus of the odd-mode reflection transfer function is, from (1),

$$|S_R(S)|^2_{\text{ODD}} = 1 - |S_T(S)|^2_{\text{ODD}} \qquad (5)$$

which can be redefined in terms of $K(S)$ as

$$|S_R(S)|^2_{\text{ODD}} = \frac{|K(S)|^2}{1 + |K(S)|^2}. \qquad (6)$$

$S_R(S)$ may then be found with the knowledge of

$$|S_R(S)|^2_{\text{ODD}} = S_R(S)|_{\text{ODD}} \cdot S_R(-S)|_{\text{ODD}}. \qquad (7)$$

From this, the input impedance of the odd-mode prototype can then be derived in a 1-Ω system using

$$Z_{\text{in}}(S)|_{\text{ODD}} = \frac{1 + S_R(S)|_{\text{ODD}}}{1 - S_R(S)|_{\text{ODD}}} \qquad (8)$$

and then synthesized using standard element extraction.

A possible source of CMRR degradation in Class-A networks is the leakage of common-mode energy through the network. This is particularly a concern in inhomogeneous media such as microstrip or coplanar waveguide. To investigate this further,

consider the inhomogeneous transfer admittance of the isolating section [the dashed box in Fig. 2(c)] [7]

$$Y_{12} = -j \frac{\cos(\theta_e) - \cos(\theta_o)}{Z_{oe}\sin(\theta_o)\cos(\theta_e) + Z_{oe}\cos(\theta_o)\sin(\theta_e)} = Y_{21} \qquad (9)$$

where Z_{oe} and Z_{oo} are the even- and odd-mode impedances of the coupled lines and θ_e and θ_o are the even- and odd-mode phase lengths, respectively. It is seen from (9) that the numerator is zero only when the even- and odd-mode phase lengths are equal, resulting in the equivalence of Fig. 2(c). Thus, the deterioration in sub-system performance due to the inhomogeneous media will be manifested in lower achievable CMRR since the transmission of the even-mode network $|S_T(S)|^2_{\text{EVEN}}$ will have a finite value.

B. Class-B Network

Another four-port circuit with valuable characteristics is the quadrature coupler of Fig. 4(a) with even- and odd-mode prototypes illustrated in Fig. 4(b) and (c). The even- and odd-mode prototypes consist typically of sections of shunt eighth-wavelength open- and short-circuited stubs, respectively, separated by quarter-wavelength-long sections of transmission lines of uniform impedance Z_i. Each quarter-wave transmission-line section may then be split into two equal sections and the resulting $ABCD$ matrix of a cascade pair of eighth-wavelength transmission lines is

$$\begin{bmatrix} A & B \\ C & D \end{bmatrix} = \left\{ \frac{1}{\sqrt{1-S^2}} \begin{bmatrix} 1 & \dfrac{S}{Z_i} \\ Z_i S & 1 \end{bmatrix} \right\}^2$$

$$= \frac{1}{1-S^2} \begin{bmatrix} 1+S^2 & \dfrac{2S}{Z_i} \\ 2Z_i S & 1+S^2 \end{bmatrix}. \qquad (10)$$

From (10), it is seen that the resulting matrix is invariant with respect to the transformation

$$S \rightarrow \frac{1}{S} \qquad (11)$$

except for a change of sign [8]. This leads to a very interesting property. The above implies that the odd-mode prototype of the coupler can be driven from its even mode, and vice versa, by simply replacing the open-circuited stubs by short-circuited stubs [8]. Now in the S-plane, the even- and odd-mode prototypes have low-pass and high-pass responses, respectively. In the f-plane, the low-pass and high-pass responses become periodic functions with bandstop and bandpass responses, respectively, at the center frequency f_o. Thus, over a frequency band centered at f_o, the even-mode network suppresses common-mode signals, while the odd-mode prototype passes differential-mode signals. Thus, the CMRR of this network has the relationship already defined in (3). In this case, the square of modulus of the even-mode transmission transfer function $|S_T(S)|^2_{\text{EVEN}}$ only dips to zero at the center of the band and, thus, the CMRR will have a varying characteristic with enhanced performance in the middle of the operating band.

The quadrature coupler utilized as an inter-stage network has a maximum bandwidth ratio (f_2/f_1 : 1 where f_1 and f_2 are the passband edge frequencies) of 3 : 1 over which there is discrimination of common- and differential-mode signals. This condition is satisfied only if the cutoff frequency f_1 of the even-mode prototype is chosen to be

$$f_1 = \frac{f_o}{2} \qquad (12)$$

leading to an upper cutoff frequency of

$$f_2 = 3f_1. \qquad (13)$$

Thus, in principle, the quadrature coupler could be used as an inter-stage network, but in contrast to a Class-A network, it is a low-pass structure. This structure can be modified for the purpose of biasing active devices with the inclusion of a pair of wide-band bias T's [9] at the input arms. However, by proper selection of the relevant set of transmission zeros, a coupler-like network that supports dc bias can be designed. This leads to the Class-B inter-stage network shown in Fig. 5. The generalized odd-mode S-plane prototype of a Class-B circuit is illustrated in Fig. 5(b) and consists of a minimum of five zeros at dc and i UEs, where i is an even number to maintain physical symmetry [11]. This has the benefit of providing dc bias to other parts of the system if required. It is now intuitive to conclude that the even- and odd-mode sub-networks of the coupler-like network will provide the necessary attenuation and matching of common- and differential-mode signals. This is illustrated in Fig. 6 for a set of synthesized Class-B prototypes with a 3 : 1 passband centered at 500 MHz, for various filter degrees. It is seen that the even- and odd-mode responses are considerably different from each other over the frequency range of interest. The main advantage of a Class-B network is simplicity in design, control of the even-mode attenuation level, and inherent broad-band operation. It is worth pointing out that the effective
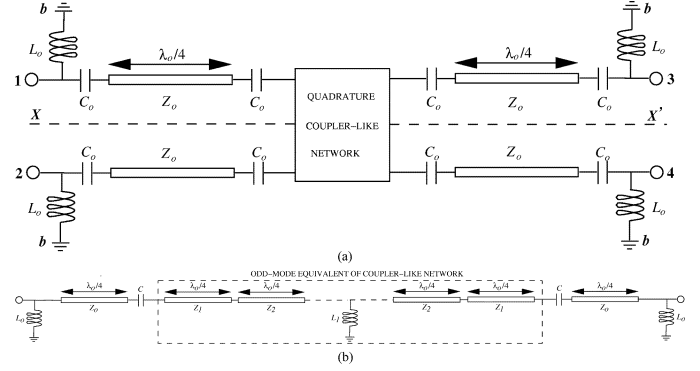
Fig. 5.   Generalized topology of Class-B inter-stage network. (a) Physical topology. (b) Odd-mode prototype with five zeros at dc and i UEs ($i = 4, 6, 8, 10, \ldots$).

(a)

(b)
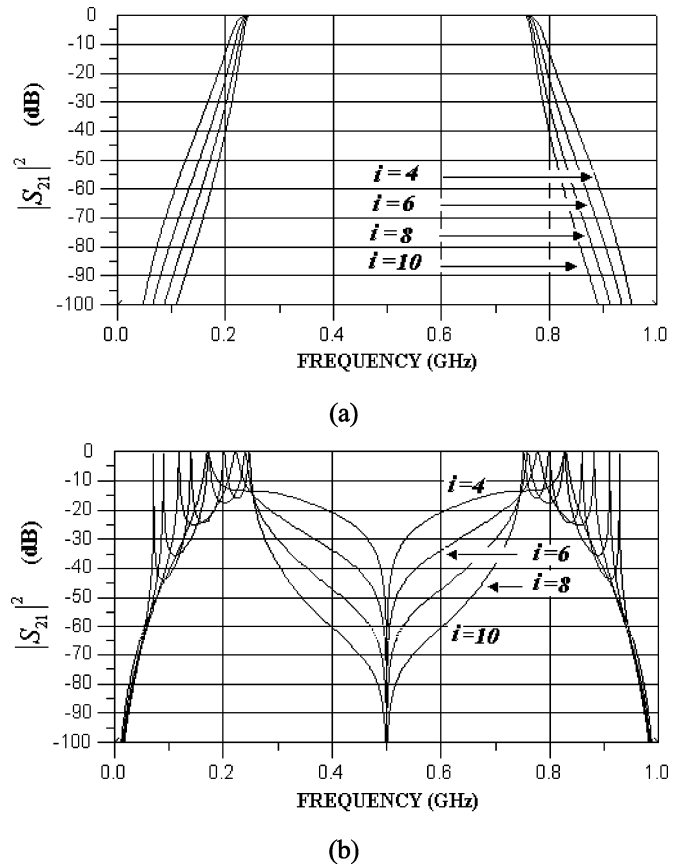
Fig. 6.   Simulated transmission characteristics of Class-B inter-stage network for different degrees. (a) Odd- and (b) even-mode responses centered at 500 MHz with a 3 : 1 bandwidth.

electrical lengths of the transmission lines forming the branches of the coupler-like section of Class-B networks are a half-wavelength long, whereas the branches of the true quadrature coupler are a quarter-wavelength long. In general, Class-B networks are particularly suited for systems operating at very high frequency, as electrical miniaturization of a Class-B structure is not possible, as it is the case with Class-A networks.

III. EXPERIMENTAL RESULTS

Experimental implementations of the two classes of inter-stage networks will now be presented.

A. Implementation of a Class-A Inter-Stage Network

A pseudodifferential amplifier (HELA-10B)[1] was selected and integrated with a Class-A network. The amplifier has a gain of 11 dB and broad-band operation from 50 MHz to 1 GHz in a 50-Ω system. The chip requires a single +12-V dc power supply.

An odd-mode S-plane bandpass filter prototype was designed corresponding to an f-plane response with a center frequency, f_o of 500 MHz, band-edge frequencies (f_1 and f_2) of 250 and 750 MHz, a commensurate frequency f_r of 2 GHz, and a return loss (RL) of 16 dB. The set of transmission zeros chosen for this filter are three zeros at dc, three zeros at infinity, and two nonredundant UEs. Based on this, the characteristic polynomial $K(S)$ of the filter prototype is constructed using a classic procedure [4], [10]. This gives

$$K(S) = \frac{(2S\sqrt{1-S^2})}{\begin{pmatrix} -56.51122588S^4 + 0.01613466S^3 \\ -13.39620723S^2 + 0.0001404614S \\ -0.629533102 \end{pmatrix}} \quad (14)$$

from which the input reflection coefficient is evaluated using (6) and (7) leading to

$$S_R(S)|_{\text{ODD}} = \frac{\begin{pmatrix} -56.51122588S^4 + 0.01613466S^3 \\ -13.39620723S^2 + 0.0001404614S \\ -0.629533102 \end{pmatrix}}{\begin{pmatrix} 56.51122588S^4 + 23.2890949S^3 \\ +18.19509163S^2 + 3.1689416S \\ +0.629533102 \end{pmatrix}}. \quad (15)$$

The input impedance $Z_{\text{in}}(S)|_{\text{ODD}}$ was then evaluated using (8). The synthesized prototype is shown in Fig. 7(a) in a 50-Ω system. Construction of the four-port inter-stage network is now possible after transformation of parts of the odd-mode prototype to a structure made of coupled lines and lumped capacitors. Fig. 7(b) shows the final layout.

Implementation on an FR4 board with a substrate thickness of 62 mil (1.57 mm), relative dielectric constant of 4.7, and loss tangent of 0.016 translate coupled-line even- and odd-mode impedances of 276.589 and 48.69 Ω to a pair of transmission line that are 10-mil (0.254 mm) wide and 7-mil (0.177 mm) apart. The coupled lines are 910-mil (23.114 mm) long. These dimensions were obtained using Agilent's Advanced Design Tool (ADS).[2] The even- and odd-mode transmission characteristics of the physical layout of Fig. 7(b) were measured, and are presented in Fig. 7(c). It is clear that there is an appreciable difference between the two responses, as predicted by the theory. In the odd mode, a bandpass response of 3 : 1 bandwidth ratio is observed when the even-mode isolation is at least 22 dB. The finite even-mode isolation level is primarily due to the difference between the even- and odd-mode phase velocities of the microstrip media leading to the transmission of
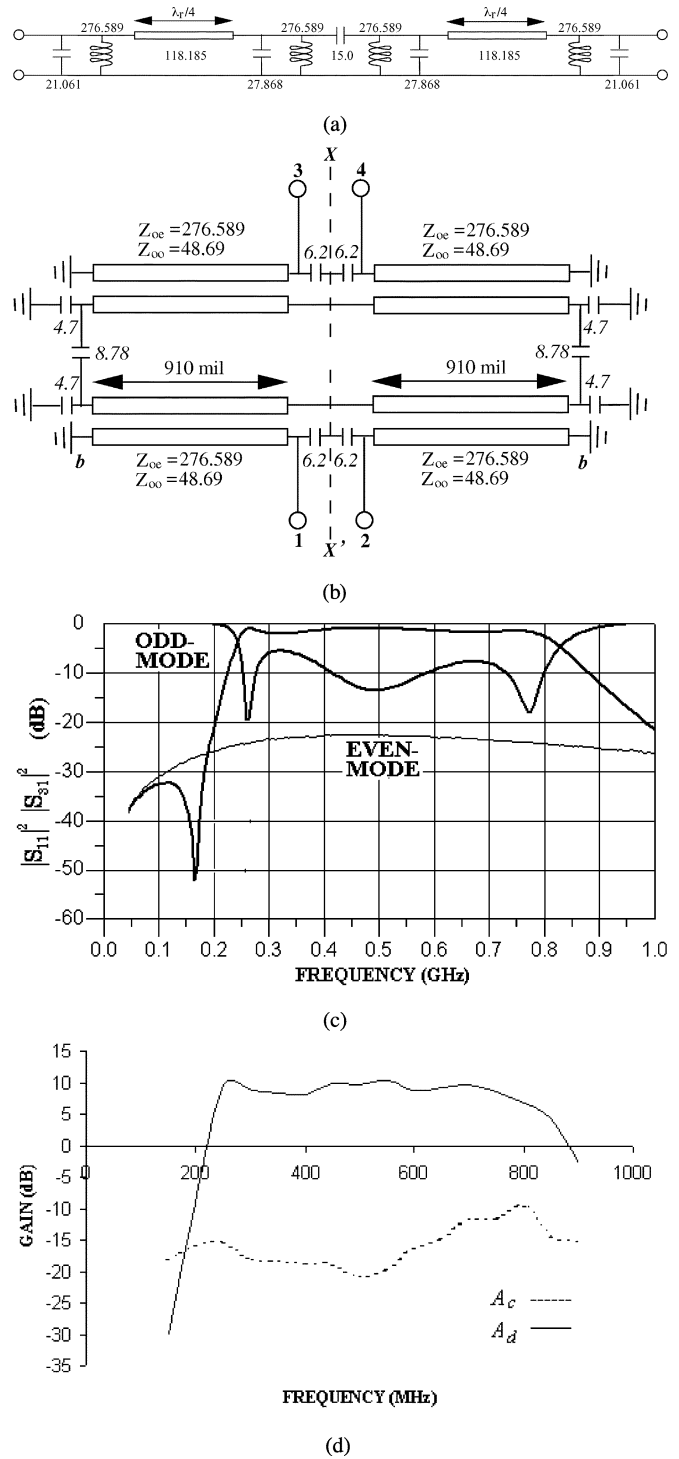
Fig. 7. Class-A inter-stage network in a 50-Ω system. (a) Synthesized odd-mode prototype. (b) Physical layout loaded with lumped capacitors in picofarads. (c) Measured even- and odd-mode transmission characteristics of (b). (d) Measured common- and differential-mode gains of sub-system configuration comprising pseudodifferential amplifier in cascade with the inter-stage network.

common-mode signals through the isolating sections, as discussed in Section II. Another source of energy leakage contributing to this finite isolation level is the parasitic coupling beyond nearest neighboring resonators leading to unwanted couplings throughout the even-mode networks of the inter-stage

network. This is particularly true since there is very weak coupling between closely spaced pairs of resonators of isolating sections giving rise to crosscoupling routes.

At this point, the pseudodifferential amplifier and inter-stage network were integrated and the overall characteristics measured. The result is shown in Fig. 6(d). Very low common-mode gain A_c of less than -12 dB was recorded over the operating bandwidth while a $3:1$ bandwidth ratio was achieved with a differential-mode gain A_d of approximately 10 dB. The excess 1 dB of loss is attributed to loss in the inter-stage network. Also, it is observed that the differential-mode gain ripples over the measured passband and rolls off rapidly toward the upper band edge frequency, i.e., 750 MHz. This is primarily due to the impedance-level mismatches since the measured RL of the inter-stage circuit is only 6 dB [see Fig. 7(c)]. The deteriorated RL was due to the restriction imposed by the FR4 board manufacturing process that only allowed a minimum of 7-mil spacing between the coupled lines. To achieve a better RL, e.g., 12 dB, a 5-mil spacing between the lines is required.

B. Implementation of a Class-B Inter-Stage Network

A Class-B inter-stage network was also designed on an FR4 board with the same specification to that used in Section III-A. In this case, the objective is to highlight the characteristics of the even- and odd-mode networks of a Class-B circuit without integration with the pseudodifferential amplifier. The odd-mode prototype was designed for an f-plane response identical to that defined in Section III-A, but with an RL of 36 dB. Here, the commensurate frequency f_r of the f-plane prototype coincides with the center frequency f_o since the prototype corresponds to an S-plane high pass. The set of transmission zeros of the odd-mode prototype of the coupler-like network are chosen to be five zeros at dc and four UEs. The characteristic polynomial $K(S)$ was directly generated using [11] to give

$$K(S) = \frac{\begin{pmatrix} -.3234410760S^{12} - 4.831961462S^{10} \\ -12.43391743S^8 + 6.369465650S^6 \\ +29.01088612S^4 - 1.294045780S^2 \\ -16.49698604 \end{pmatrix}}{2S^5(S^2-1)}. \quad (16)$$

In a manner similar to that used previously, $S_R(S)|_{\text{ODD}}$ and $Z_{\text{in}}(S)|_{\text{ODD}}$ are constructed using (6)–(8).

Direct synthesis of the above transfer function leads to the prototype of Fig. 8(a). Application of the appropriate Kuroda transformations to the circuit of Fig. 8(a) results in the circuit of Fig. 8(b). It is seen from Fig. 8(b) that the characteristic impedance of the inner pair of shunt short-circuited stubs are of value 33.27 Ω. This pair of stubs was forced to have a value of 50 Ω by application of some circuit optimization leading to a degradation of the RL from 36 dB to approximately 15 dB with a slight increase in bandwidth. This is acceptable since there was a lot of RL to factor. The prototype is shown in Fig. 8(c). At this point, the layout of the inter-stage network was constructed from the odd-mode prototype, as illustrated in Fig. 8(d). However, the input and output sections (series open-circuited stubs separated by a UE) are difficult to realize using microstrip technology and equivalence to coupled lines must be made
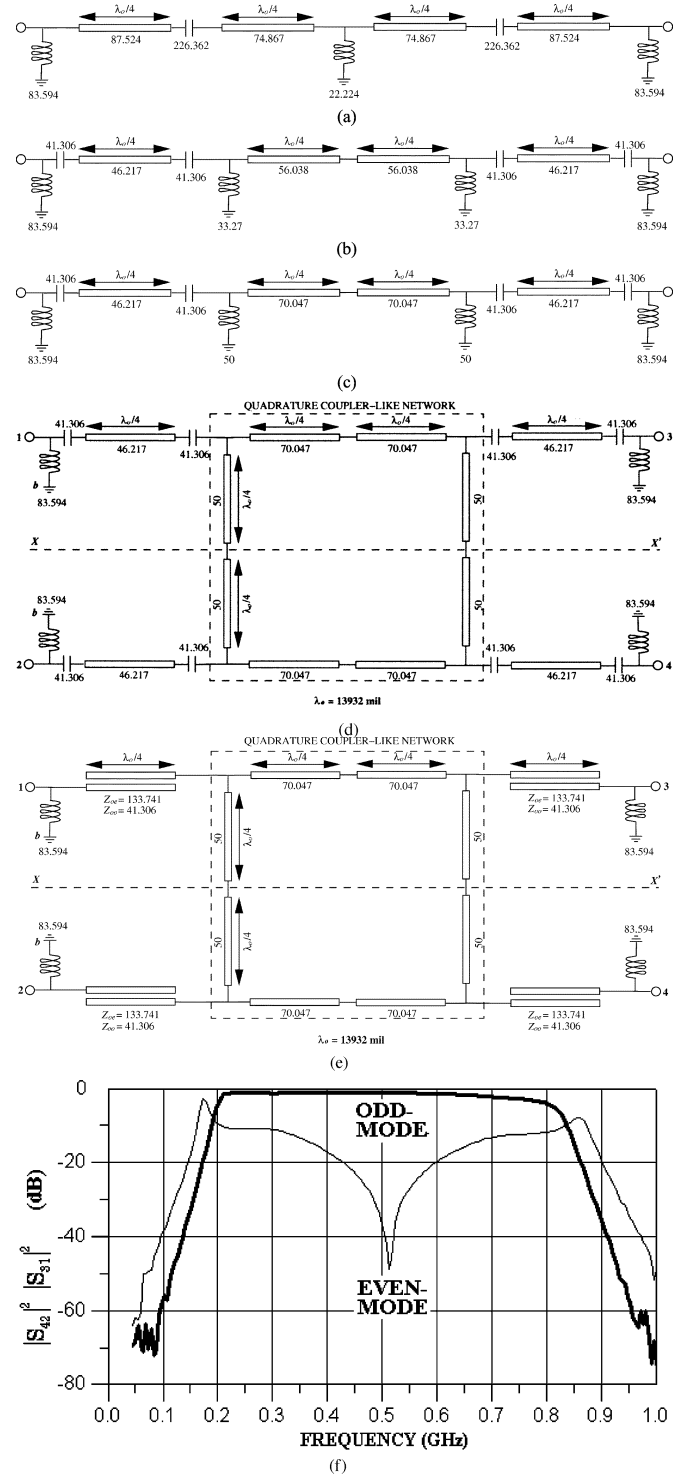
Fig. 8. Class-B inter-stage network in a 50-Ω system. (a) Synthesized odd-mode prototype. (b) After application of relevant Kuroda transformations. (c) After some circuit optimization. (d) and (e) Physical layout. (f) Measured even- and odd-mode transmission characteristics of the circuit of (e).

leading to the final network of Fig. 8(e). Now the even- and odd-mode impedances of values 133.741 and 41.306 Ω of each coupled-line section were then translated into physical dimensions resulting in a width of 27 mil (0.685 mm), spacing of 7 mil (0.177 mm), and length of 3483 mil (88.468 mm). The width of the other transmission lines of 50, 70.047, and 83.594 Ω were 110 (2.794 mm), 57 (1.447 mm), and 38 mil

(0.965 mm), respectively. The lengths of all the transmission lines were also 3483 mil (88.468 mm).

The measured even- and odd-mode transmission characteristics of the inter-stage network are shown in Fig. 8(f), showing significant difference, as expected.

IV. CONCLUSION

This paper has presented the derivation and design procedures of two new classes of four-port microwave inter-stage networks that choke common-mode signals over a very broad frequency range. The design procedure presented for the new networks is based on the synthesis of an odd-mode matching/filtering prototype with broad bandwidth and out-of-band rejection levels. Subsequent integration of either class of these networks with pseudodifferential circuits leads to dramatic improvement of the sub-system CMRR over very large bandwidth. This improvement was demonstrated experimentally. Both classes of networks possess fundamentally different even- and odd-mode transmission characteristics and reflect undesired common-mode energy. Class-B networks could be designed to posses a finite attenuation level to reject common-mode signals. This feature does not exist with Class-A networks and basically the rejection level of common-mode signals will depend on how homogeneous the realization media is. Choice of which class to use is dependent on the system application and on the evaluated strengths of undesired common-mode signals.

REFERENCES

[1] W. M. Fathelbab and M. B. Steer, "Distributed biasing of differential RF circuits," *IEEE Trans. Microw. Theory Tech.*, vol. 52, no. 5, pp. 1565–1572, May 2004.

[2] G. Matthaei, L. Young, and E. M. T. Jones, *Microwave Filters Impedance-Matching Networks, and Coupling Structures*. Norwood, MA: Artech House, 1980.

[3] R. Mongia, I. Bahl, and P. Bhartia, *RF and Microwave Coupled-Line Circuits*. Norwood, MA: Artech House, 1999.

[4] R. J. Wenzel, "Synthesis of combline and capacitively loaded interdigital bandpass filters of arbitrary bandwidth," *IEEE Trans. Microw. Theory Tech.*, vol. MTT-19, no. 8, pp. 678–686, Aug. 1971.

[5] I. Hunter, *Theory and Design of Microwave Filters*. London, U.K.: IEE Press, 2001.

[6] H. Ozaki and J. Ishii, "Synthesis of a class of strip-line filters," *IRE Trans. Circuit Theory*, vol. CT-5, pp. 104–109, Jun. 1958.

[7] G. I. Zysman and A. K. Johnson, "Coupled transmission line networks in an inhomogeneous dielectric medium," *IEEE Trans. Microw. Theory Tech.*, vol. MTT-17, no. 10, pp. 753–759, Oct. 1969.

[8] R. Levy and L. F. Lind, "Synthesis of symmetrical branch-guide directional couplers," *IEEE Trans. Microw. Theory Tech.*, vol. MTT-16, no. 2, pp. 80–89, Feb. 1968.

[9] B. J. Minnis, "Decade bandwidth bias Ts for MIC applications up to 50 GHz," *IEEE Trans. Microw. Theory Tech.*, vol. MTT-35, no. 6, pp. 597–600, Jun. 1987.

[10] H. J. Orchard and G. C. Temes, "Filter design using transformed variable," *IEEE Trans. Circuit Theory*, vol. 15, pp. 385–408, Dec. 1968.

[11] M. Horton and R. Wenzel, "General theory and design of optimum quarter-wave TEM filters," *IEEE Trans. Microw. Theory Tech.*, vol. MTT-13, no. 5, pp. 316–327, May 1965.

Wael M. Fathelbab (M'03) received the Bachelor of Engineering (B.Eng.) and Doctor of Philosophy (Ph.D.) degrees from the University of Bradford, Bradford, U.K., in 1995, and 1999 respectively.

From 1999 to 2001, he was an RF Engineer with Filtronic Comtek (U.K.) Ltd., where he was involved in the design and development of filters and multiplexers for various cellular base-station applications. He was subsequently involved with the design of novel RF front-end transceivers for the U.K. market with the Mobile Handset Division, NEC Technologies (U.K.) Ltd. He is currently a Research Associate with the Department of Electrical and Computer Engineering, North Carolina State University, Raleigh. His research interests include network filter theory, synthesis of passive and tunable microwave devices, and the design of broad-band matching circuits.

Michael B. Steer (S'76–M'82–SM'90–F'99) received the B.E. and Ph.D. degrees in electrical engineering from the University of Queensland, Brisbane, Australia, in 1976 and 1983, respectively.

He is currently a Professor with the Department of Electrical and Computer Engineering, North Carolina State University, Raleigh. In 1999 and 2000, he was a Professor with the School of Electronic and Electrical Engineering, The University of Leeds, where he held the Chair in microwave and millimeter-wave electronics. He was also Director of the Institute of Microwaves and Photonics, The University of Leeds. He has authored over 260 publications on topics related to RF, microwave and millimeter-wave systems, high-speed digital design, and RF and microwave design methodology and circuit simulation. He coauthored *Foundations of Interconnect and Microstrip Design* (New York: Wiley, 2000).

Prof. Steer is active in the IEEE Microwave Theory and Techniques Society (IEEE MTT-S). In 1997, he was secretary of the IEEE MTT-S. From 1998 to 2000, he was an elected member of its Administrative Committee. He is the Editor-in-Chief of the IEEE TRANSACTIONS ON MICROWAVE THEORY AND TECHNIQUES (2003–2006). He was a 1987 Presidential Young Investigator (USA). In 1994 and 1996, he was the recipient of the Bronze Medallion presented by the Army Research Office for "Outstanding Scientific Accomplishment." He was also the recipient of the 2003 Alcoa Foundation Distinguished Research Award presented by North Carolina State University.